J. Fluid Mech. (1972), *vol.* 51, *part* 4, *pp.* 625–635
Printed in Great Britain

Solitary waves in concentrated vortices

By S. LEIBOVICH AND J. D. RANDALL
Department of Thermal Engineering, Cornell University, Ithaca, N.Y.

(Received 26 July 1971)

A nonlinear integro-differential equation governing finite amplitude wave propagation on concentrated vortices is solved numerically. The solution to the Cauchy problem shows a solitary wave development qualitatively similar to solutions of the Korteweg–de Vries equation. A perturbation solution of the stationary form of the evolution equation confirms the unsteady calculation.

1. Introduction

It has been shown earlier (Leibovich 1970) that a nonlinear integro-differential equation governs the evolution of small finite amplitude wave motions propagating on concentrated vortices. This equation may be written in the form

$$A_t = c_1 A A_x + c_3 \frac{\partial^3}{\partial x^3}\left\{A + \left(2\ln\frac{1}{k}\right)^{-1}\int_{-\infty}^{\infty} \ln(2|x-\xi|)\,\mathrm{sgn}\,(x-\xi)\,A_\xi\,d\xi\right\}, \qquad (1)$$

where c_1 and c_3 are constants given in the paper cited†. The equation arises in an approximation procedure which requires k (which plays the role of a wavenumber) to be small. For the stationary case Pritchard (1970) has presented an equivalent equation.

For $k = 0$, (1) reduces to the Korteweg–de Vries equation, which admits solitary wave solutions. One presumes that such disturbances are possible for $k > 0$, but this requires verification. This question is explored in the present note in two ways. The first approach, which represents the major effort, consists of numerical solutions of the Cauchy problem for (1) for various values of the parameter $(2\ln(1/k))^{-1}$, to which we assign the label β. The initial condition chosen is one for which exact results for the Korteweg–de Vries case $\beta = 0$ are known (Zabusky 1968), and we are therefore able to compare our results with an exact solution.

For β, small solutions are qualitatively much like those in the Korteweg–de Vries case. The initial distribution breaks up into two (separating) solitary waves and an oscillatory tail that travels in the opposite direction. The shape, speed and distribution of

$$\text{'momentum'}\left(\int_{-\infty}^{\infty} A(x,t)\,dx\right) \quad \text{and} \quad \text{'energy'}\left(\int_{-\infty}^{\infty} \tfrac{1}{2}A^2(x,t)\,dx\right)$$

of the emerging solitary waves differ from the Korteweg–de Vries case, but nearly

† This is the required form in physical (x, t) space of Leibovich's (1970) equation (27), which is the Fourier transform of (1). Equation (28) of that paper is obtained from (27) by an *ad hoc*, but asymptotically equivalent, replacement of certain terms.

all the energy and most of the momentum of the wave systems continues to be transported by the solitary waves. As β increases, the differences, of course, increase and for sufficiently large β (between 0·25 and 0·33) qualitatively different results are found and are explored for $\beta = 0{\cdot}5$.

Our second approach consists of the direct construction of solitary waves by means of a perturbation solution (for small β) of the stationary form of (1). The results closely confirm the transient calculations and show that, compared to a Korteweg–de Vries solitary wave of the same amplitude, the $\beta > 0$ waves are narrower and slower. This is consistent with the formula for solitary wave speeds

$$c_s = c_1 E_s / M_s,$$

derived by Benjamin (private communication) for dispersive equations more general than (1). (Integrals for energy and momentum are taken over individual solitary waves.)

It therefore appears that the model of wave propagation on concentrated vortices incorporated in (1) does contain the possibility of solitary waves. Experimental evidence to this effect is already conclusive (Pritchard 1970), but is not sufficiently detailed to permit a comparison with the present results.

2. The equation governing wave development

The values of the coefficients c_1 and c_3, although fixed by the particular vortex motion under consideration and important in the calculation of the stream function are irrelevant to the solution of (1). For if the substitutions (note that $c_3 > 0$)

$$t = c_3^{-1} T,$$

$$A = (\alpha c_3 / c_1)\, U(x, T)$$

are made in (1), dependence on c_1 and c_3 is removed. The coefficient α may be chosen arbitrarily and is inserted for convenience.

It is worth noting at this point that the maximum amplitude $A_{\max}$ may be arbitrary without violating the small disturbance assumptions giving rise to equation (1). This is important, since we shall later take the initial amplitude of U to be 5 and $\alpha = 6$, and so $A_{\max}$ is potentially rather large (depending on c_3/c_1). According to the derivation by Leibovich (1970), however, the perturbations are of order $\epsilon A_{\max}$, where ϵ is an adjustable small parameter. Thus $A_{\max}$ is arbitrary, although its product with ϵ must be small.

We introduce the 'momentum'

$$M(T) = \int_{-\infty}^{\infty} U(x, T)\, dx$$

and the 'energy'

$$E(T) = \int_{-\infty}^{\infty} \tfrac{1}{2} U^2(x, T)\, dx.$$

As indicated below, (1) (now in terms of U and T) has the conservation properties

$$dM/dT = dE/dT = 0,$$

provided that $M(0) < \infty$ and $E(0) < \infty$. Such conservation laws serve as useful checks on the numerical calculation. In fact, our numerical algorithms are carefully constructed to be inherently compatible with energy and momentum conservation.

Conservation of M follows simply by integrating (1) over all x. To show that E is conserved, multiply (1) by U and integrate over x to obtain

$$\frac{dE}{dT} = \beta \iint_{-\infty}^{\infty} U_{xx}(x, T)\, U_{\xi\xi}(\xi, T) \ln (2|x-\xi|) \operatorname{sgn}(x-\xi)\, dx\, d\xi$$

after three integrations by parts and application of the boundary condition $U \to 0$ as $x \to \infty$. In the x, ξ plane the integrand is antisymmetric about the line $x = \xi$ and hence the integral over the plane vanishes, giving the desired result. Actually, M and E are directly related to the total disturbance axial momentum and kinetic energy in the vortex core, but the connexion is not important here.

To conclude this section, note that by repeated integration by parts followed by differentiation, and by use of the scalings introduced in this section, the governing equation (1) may be written in the form

$$U_T = \alpha U U_x + U_{xxx} + \beta \int_{-\infty}^{\infty} \ln (2|x-\xi|) \operatorname{sgn}(x-\xi)\, U_{\xi\xi\xi\xi}\, d\xi, \qquad (2)$$

which is approximated by finite differences in the next section.

3. Numerical procedure

Let h_x be the step in x from the spatial grid point i to its neighbour, $i+1$, and let h_τ be the time step from time level n to time level $n+1$. The following 3 time-level explicit finite-difference formula is stable, compatible with (2) and conserves energy and momentum.

$$\begin{aligned}(U_i^{n+1} - U_i^{n-1})/2h_\tau = {} & (\alpha/30h_x)\,(U_{i+2}^n + U_{i+1}^n + U_i^n + U_{i-1}^n + U_{i-2}^n) \\ & \times (U_{i+2}^n + U_{i+1}^n - U_{i-1}^n - U_{i-2}^n) \\ & + (1/2h_x^3)\,(U_{i+2}^n - 2U_{i+1}^n + 2U_{i-1}^n - U_{i-2}^n) \\ & + \beta h_x^{-3} \sum_{j=1}^{N} W(i-j)\,(U_{j+2}^n - 4U_{j+1}^n + 6U_j^n - 4U_{j-1}^n + U_{j-2}^n) \\ & + T_E + Q. \end{aligned} \qquad (3)$$

The weight function $W(i-j)$ is discussed later. T_E is the truncation error associated with the difference approximations to derivatives and Q represents the various errors involved in the replacement of the integral by the numerical quadrature. The truncation error may easily be shown to be $O(h_\tau^2) + O(h_x^2)$. The quadrature formula and quadrature error Q require some elaboration, since difficulties due to the infinite range of integration and to the singular nature of the kernel arise. A brief discussion is included in the appendix.

Consider first the errors associated with a truncated range of integration.

Initially, the disturbances will be, by hypothesis, localized near $x = 0$. In fact, initial data is chosen to be of solitary wave form and decreases exponentially as $|x|$ increases. Experience with the Korteweg–de Vries equation (Zabusky 1968) shows that the initial distribution breaks up into solitary waves moving at a definite finite speed, and a small amplitude oscillation moving in the opposite direction with the group velocity for infinitesimal waves. Thus the disturbed region grows linearly with time, but for finite time is bounded, and outside this region of disturbance U is exponentially small.

A similar picture holds for equation (2), but the integral term spreads the disturbance effect over a larger region, causing the decay at large distances to be algebraic. In fact, it can be shown (Randall 1972) that the integral term behaves like $24\,\mathrm{sgn}\,xM(0)\,x^{-4}$ as $|x| \rightarrow \infty$. The integral is truncated on the left at $x = L_1$ and on the right at $x = L_2$ in the numerical work. Our procedure is to choose L_1 and L_2 to ensure that $24M(0)/L_1^4$ and $24M(0)/L_2^4$ are smaller by about two orders of magnitude than the other sources of error permitted in the calculation. This necessitates increasing L_1 and L_2 occasionally as the disturbance region grows. When this was done the values of U were set equal to zero at the new grid points. They became non-zero, but small, as the calculation resumed. For the worst case, $\beta = 0{\cdot}1$, it was found that the grid had to be periodically enlarged from an initial size of 301 points to 401 points in the time interval of the computation. A von Neumann stability analysis of the linearized version of (2) indicates stability if the time and space increments are chosen so that $h_\tau \leqslant 2h_x^3/\sqrt{27}$ if $\beta = 0$. For $\beta > 0$ the condition is more stringent, but $h_\tau = h_x^3/\sqrt{27}$ was found to be satisfactory in practice.

Zabusky (1968) has investigated solutions of the Korteweg–de Vries equation subject to the initial condition†

$$U(x,0) = p(p+1)\,\mathrm{sech}^2\,x. \tag{4}$$

Since several properties of the time-dependent solution of the Korteweg–de Vries equation corresponding to this initial condition are well known we have adopted it for the present work, with $p(p+1) = 5$. In order to start our calculation one must know both $U(x,0)$ and $U(x,h_\tau)$. We take

$$U(x,h_\tau) = 5\,\mathrm{sech}^2\,(x+ch_\tau),$$

where $c = \alpha E(0)/M(0)$ is the speed of propagation of a solitary wave with the same energy and momentum as the initial distribution.

The step size used in most of our calculations was $h_x = 0{\cdot}1$. In computations using this mesh, energy fluctuations remained less than $0{\cdot}18\,\%$ of the initial energy, and momentum deviated by less than $0{\cdot}73\,\%$ of its initial value. With this mesh size it was found that a calculation for a single value of β which ran for a time sufficient to clearly distinguish the ultimate steady system of permanent waves (about 2400 time steps) required about an hour and a half on an IBM 360/65. Furthermore, computation time is generally proportional to N^5, where N is the number of mesh points. Calculations with reduced step sizes to check convergence

† Zabusky treated solitary waves of negative amplitude, and so there are inconsequential differences in sign between his work and ours.

of the algorithm are therefore very expensive. We have been content with a computation using a step size $h_x = 0{\cdot}075$, running for 1185 time steps with $\beta = 0{\cdot}1$. This is comparable to the time level reached after 500 steps with $h_x = 0{\cdot}1$. The difference in the main peaks is less than 1%, while the second peaks remain within 5%. Maximum deviation in the wave form is 6·7% and occurs on the downstream side of the main peak.

4. Perturbation procedure for stationary solutions

The stationary form of (2), obtained by replacing U_T by $c_s U_x$ and integrating once, is

$$c_s U = \tfrac{1}{2}\alpha U^2 + U_{xx} + \beta \int_{-\infty}^{\infty} U_{\xi\xi\xi} \ln(2|x-\xi|)\,\mathrm{sgn}\,(x-\xi)\,d\xi. \tag{5}$$

For $\beta = 0$ the solitary wave solution is $U = a\,\mathrm{sech}^2\,\sigma x$, where $\sigma \equiv (\alpha a/12)^{\frac{1}{2}}$ and the speed is $c_s = \frac{1}{3}\alpha a$. For β small, but non-zero, a solution is sought in the form

$$\left.\begin{aligned} U &= a \sum_{n=0}^{\infty} \beta^n U_n(\eta;\, a), \\ c_s &= \tfrac{1}{3}\alpha a \sum_{n=0}^{\infty} \beta^n s_n, \end{aligned}\right\} \tag{6}$$

where $\eta = \sigma x$. Substituting (6) into (5) and equating coefficients of β^n yields

$$U_0'' + 6U_0^2 - 4s_0 U_0 = 0,$$

with solution $U_0 = \mathrm{sech}^2\,\eta$, $s_0 = 1$, and

$$U_n'' + (12U_0 - 4)\,U_n = 4s_n U_0 - G_n, \tag{7}$$

where
$$G_1 \equiv (2\ln 2\sigma^{-1})\,U_0'' + I_0,$$
$$G_n \equiv (2\ln 2\sigma^{-1})\,U_{n-1}'' + I_{n-1} + \sum_{l=1}^{n-1} (6U_{n-l} - 4s_{n-l})\,U_l, \quad n \geqslant 2,$$
and
$$I_m \equiv \int_{-\infty}^{\infty} U_m'''(\eta')\ln(|\eta-\eta'|)\,\mathrm{sgn}\,(\eta-\eta')\,d\eta'.$$

The boundary conditions imposed are

$$U_n(0) = U_n(\infty) = 0 \quad (n \geqslant 1).$$

Equations (7) have the two homogeneous solutions:

$$\theta_1 = -\tfrac{1}{2}U_0' = \mathrm{sech}^2\,\eta\tanh\eta,$$
$$\theta_2 = \theta_1 \int \frac{d\eta}{\theta_1^2} = \tfrac{1}{8}\{7 + 2\sinh^2\eta + 15\,\mathrm{sech}^2\,\eta(\eta\tanh\eta - 1)\}.$$

The constants s_n are determined by the solvability condition, which gives

$$s_n = \int_0^{\infty} \theta_1(\eta)\,G_n(\eta)\,d\eta. \tag{8}$$

The solutions for the U_n are given by

$$U_n(\eta) = \int_0^{\eta} [4s_n U_0(\eta') - G_n(\eta')]\,[\theta_1(\eta')\,\theta_2(\eta) - \theta_2(\eta')\,\theta_1(\eta)]\,d\eta'. \tag{9}$$

We have computed U_1 and s_1 using this method. The integral I_0 was evaluated by the sum formula of §3, and the integrals in (8) and (9) were evaluated by the trapezoidal rule, with step sizes of 0·02 and 0·01, and over η intervals from $\eta = 0$ to $\eta = 8$ or $\eta = 10$. All runs agreed to four decimal places. Because of the form of G_1, s_1 is independent of σ, and hence of wave amplitude a, and has the value $s_1 = -0{\cdot}2590$. This shows that $c_s/\frac{1}{3}\alpha a < 1$ for $\beta > 0$ and depends chiefly upon β and not amplitude. Higher approximations ($s_n, n \geqslant 2$) do depend upon amplitude.

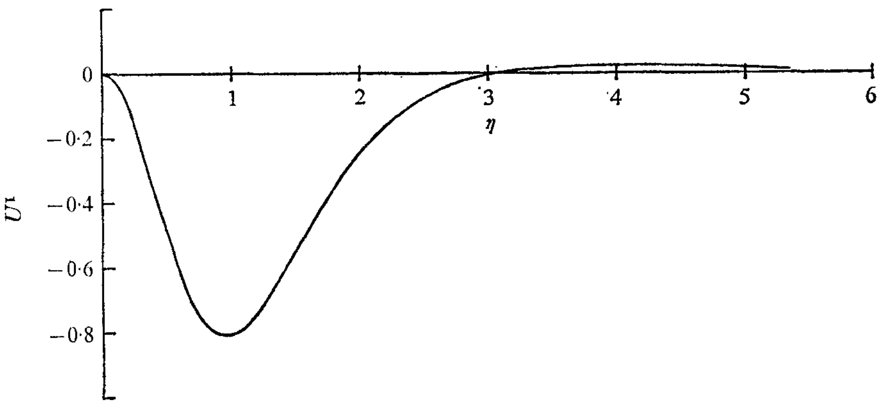

FIGURE 1. U_1 as a function of η for $\sigma = 1{\cdot}94$, corresponding to the leading solitary wave evolving for $\beta = 0{\cdot}1667$ from the unsteady calculations.

A plot of U_1 is shown in figure 1 for $a = 7{\cdot}5$ (note that as a function of η, U_1 depends only weakly upon a through the log σ term in G_1, but η itself depends upon a). Figure 1 shows that the solitary wave is narrower in the central portion and, very slightly, broader in the tail for $\beta > 0$ than the corresponding Korteweg–de Vries wave.

5. Numerical results

Equation (3) has been solved for the Korteweg–de Vries case, with $\beta = 0$, and for values of β of 0·1, 0·1667, 0·25 and 0·5, and using the constant factor $\alpha = 6$. The choice for α is arbitrary. However, the time development of the wave depends on the product of α and the initial amplitude; if this is too small the computing expense is prohibitive. Attention is directed to the emergence of solitary waves, and the computations in each case are pursued until the solitary waves are clearly defined. Before discussing the results it should be emphasized that each (stationary) solitary wave amplitude and length parameter pair (a, k) generates a continuum of other parameter pairs by defining a curve in (a, k) space, which corresponds to the same solution owing to the scaling properties of equation (5).

The Korteweg–de Vries case, $\beta = 0$, was calculated primarily to serve as a reference and as a check on our numerical procedure. The results agree with those from the GGKM theory (Gardner *et al.* 1967) and outlined by Zabusky (1968). The distribution (4) should break up into two solitary waves, with amplitudes 6·42 and 1·25 and speeds of $-12{\cdot}84$ and $-2{\cdot}50$ respectively. A small amplitude oscillating tail should spread in the positive x direction. All of these rigorous predictions are reproduced by the numerical computations within the accuracy expected from a discretized formulation. For example, the error in the main peak amplitude is 2 % and that of the second peak is 5 %, while speeds agree to within 1·4 and 3·2 % respectively.

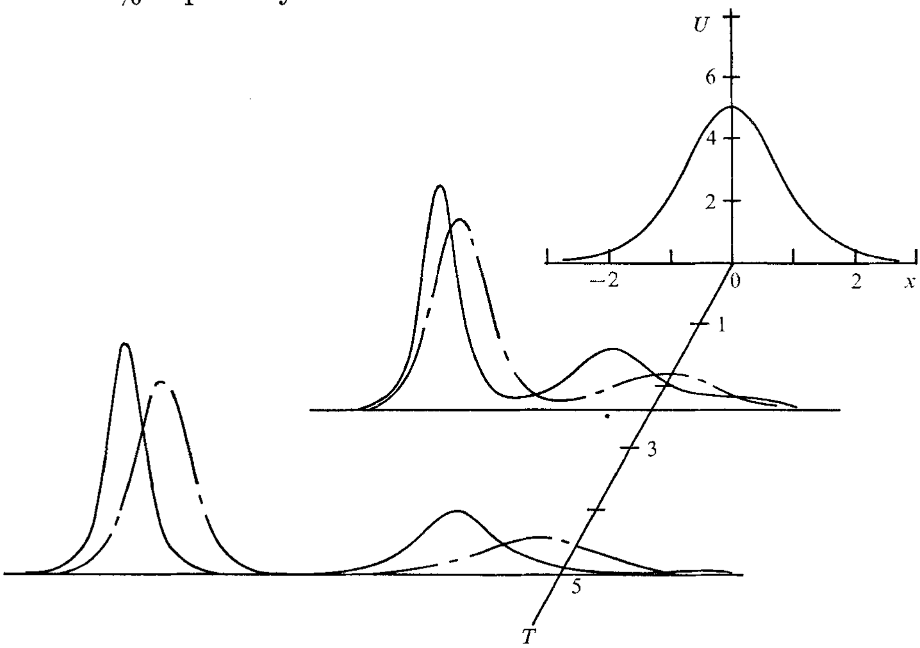

FIGURE 2. Temporal development of solitary waves for $\alpha = 6$, $U(x,0) = 5\,\mathrm{sech}^2\,x$. ——, $\beta = 0{\cdot}1667$; — · —, $\beta = 0$.

The evolution of waves of permanent form for $\beta = 0, 0{\cdot}1$ and $0{\cdot}1667$ is similar, and figure 2, summarizing the results for $\beta = 0$ and $\beta = 0{\cdot}1667$, is typical.

In all three cases the initial distribution begins to grow in amplitude and shrink in width as it moves in the negative x direction. The increase in peakedness is symmetrical, except for the splitting of a second smaller solitary wave behind the main peak. As time proceeds, the main peak separates from the smaller solitary wave and ultimately two distinct solitary waves remain. In the case of $\beta = 0{\cdot}1667$ the figure suggests the possibility that a third solitary wave may form. This is not the case. The smallest maximum in the figure in fact belongs to a small amplitude dispersing 'tail' which exists for all three of the calculations, but which is generally too small to be evident in the drawing.

Trajectories of the solitary waves and of the first few peaks of the dispersing tail are shown in figure 3. The largest solitary wave reached its permanent speed almost immediately. Identification of the small solitary wave is made long before it separates from its companion, and its speed during the gestation period is of course non-uniform. The broken lines in these figures represent the speeds that should be obtained according to the Benjamin formula mentioned earlier, i.e., the speed c_s of a solitary wave is (for equations in the T co-ordinate)

$$c_s = \alpha E_s/M_s, \tag{10}$$

where E_s and M_s are the energy and momentum of an individual solitary wave. As may be seen, there is good agreement between (10) and the solitary wave trajectories, and given the uncertainty in location of peaks (due to finite mesh size) this is probably the best way to decide speeds of solitary waves.

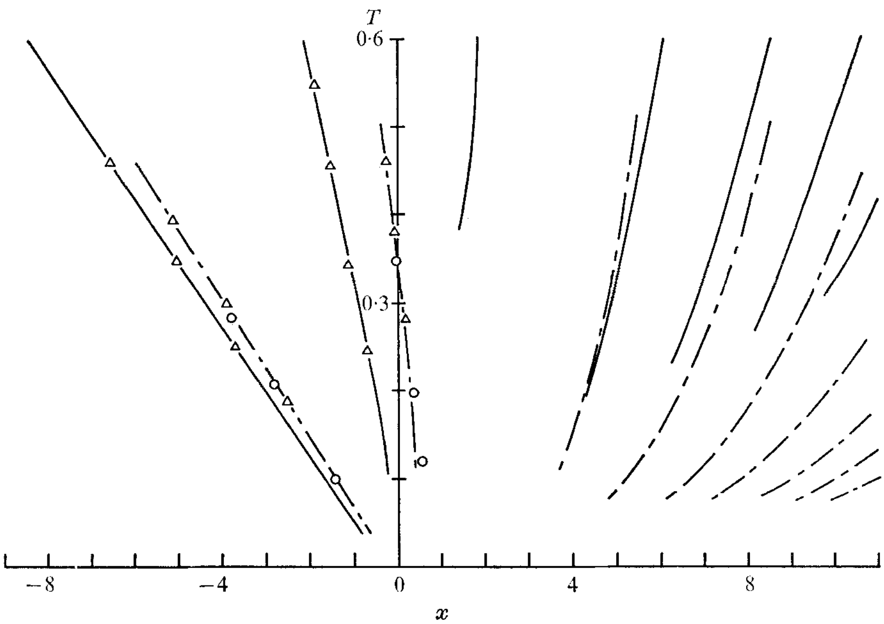

FIGURE 3. Trajectories of maxima of solitary waves (left sloping) and oscillatory tail for $\alpha = 6$, $U(x, 0) = 5\,\mathrm{sech}^2\,x$. ——, $\beta = 0{\cdot}1667$; —·—, $\beta = 0$; Δ, speeds determined from equation (10) for $\beta = 0{\cdot}1667$; ○, speeds determined from Zabusky (1968) for $\beta = 0$.

Figure 4 compares the ultimate wave forms of the leading solitary wave for $\beta = 0{\cdot}1667$ with that for a solitary wave of the *same* amplitude for $\beta = 0$. The circles are points calculated for $\beta = 0{\cdot}1667$ by the stationary solution of the preceding section. The speed for $\beta = 0{\cdot}1667$, as computed from formula (10), is 13·95. This may be compared with the corresponding result obtained by the method of §3, which produces the corresponding value of 14·35 with the next order correction expected to be of the order of β^2 or 3 %.

Although the cases $\beta = 0$ and $\beta > 0$ are similar in nature, some differences between them may be noted. The final amplitudes of the solitary wave increase and their bandwidths decrease with increasing β. Increasing proportions of the

β	% initial energy: First solitary wave	% initial energy: Second solitary wave	% initial momentum: First solitary wave	% initial momentum: Second solitary wave
0	93·28	6·66	73·8	27·6
0·1000	89·56	10·26	67·6	32·2
0·1667	85·42	14·46	61·2	35·1

TABLE 1

initial energy and momenta ultimately reside in the second solitary waves as β increases, as may be seen in table 1. Nearly all the initial energy is transported by the solitary waves (over 99·8 % for all three cases shown). The table further suggests that the momentum ultimately residing in the solitary waves decreases as β increases. For the Korteweg–de Vries case the solitary waves actually end up with more than 100 % of the initial momentum at the expense of the oscillating tail, which possesses a momentum defect. This is known to be the case

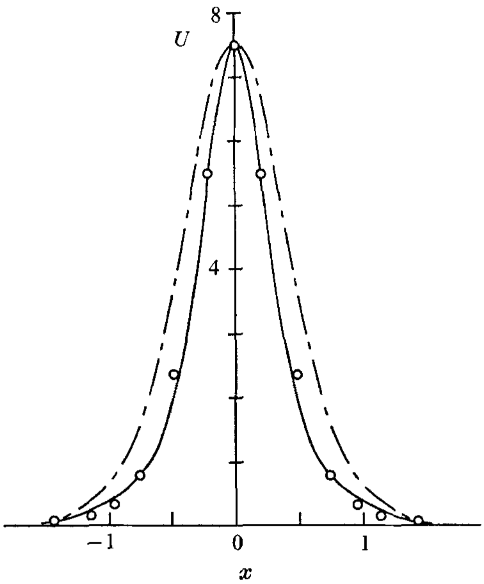

FIGURE 4. Comparison of the ultimate wave forms of the leading solitary wave for $\beta = 0{\cdot}1667$ with that for a solitary wave of the same amplitude but for $\beta = 0$. ——, leading solitary wave; —·—, solitary wave of same amplitude; ○, points computed using the perturbation method and figure 1.

from the rigorous results of Gardner *et al.* (1967) (cf. Zabusky 1968). For the present case, the exact tail energy should amount to 0·12 % of the total and there should be a 3·3 % defect in momentum. Table 1 indicates a numerical value of 0·06 % for tail energy and 1·4 % for tail momentum. In the tail, however, one is dealing with sums of very small numbers. Uncertainty in the definition of the beginning of the tail and the finite range of integration which truncates the tail are probably sufficient to explain the differences. One would expect the errors to be at least as large for $\beta > 0$ and this makes speculative any deductions of trends concerning the tails as β varies.

Our governing equation (2) is consistent with the perturbation from which it derives only if β remains small. It should be kept in mind, therefore, that the cases $\beta = 0{\cdot}25$ and $0{\cdot}50$ are very likely of no physical interest. Nevertheless, we have made computations for these cases in an attempt to gain a general understanding of the behaviour of solutions of (2) as β varies. When we put $\beta = 0{\cdot}25$ and $0{\cdot}50$, a solution with a completely different nature emerged. This new behaviour was explored in a detailed calculation for the case $\beta = 0{\cdot}50$, the results of which will be described briefly below. A short-time calculation for $\beta = 0{\cdot}25$ demonstrated the same initial behaviour and it is likely that the description below can be applied *in toto* to all values of β larger than 0·25. Instead of retaining an appearance of symmetry, the forward moving face of the main peak initially steepens and emits a sequence of smaller amplitude waves *ahead* of its own position. All waves, including the main peak, disperse and subside as time progresses, and no waves of permanent form remain. One might describe the behaviour as an attempt to generate an infinite wave train, reminiscent of the cnoidal waves of the Korteweg–de Vries equation, with only a finite amount of energy.

This anamolous behaviour is due to a frequent (in axial position) change of the sign of the term $U_T - \alpha U U_x$ caused by an increase in the magnitude of the integral term. Exactly the same kind of behaviour results from the Korteweg–de Vries equation if the sign of the third derivative is changed ($U_T = \alpha U U_x - U_{xxx}$) while keeping α and $U(x, 0)$ positive. The initial direction of motion is governed by the nonlinear term and is towards x decreasing as before. However, permanent waves cannot form, and the initial distribution breaks up and disperses as described previously. Permanent waves are possible for $\beta = 0{\cdot}50$ if the sign of α is changed (or, equivalently, the sign of $U(x, 0)$). Then rightward (x increasing) propagating wave patterns occur and are similar to the other computed cases, except that now there are more solitary waves, and each of these are bracketed by small *negative* troughs. A more detailed description of these computations is given by Randall (1972).

6. Conclusions

Our results may be summarized by the following description. An initial distribution of $U = 5\,\text{sech}^2 x$ decomposes into two solitary waves moving in the negative x direction and a small amplitude oscillating tail (assuming both positive and negative amplitudes) that propagates in the direction of x increasing. The larger solitary wave has an amplitude exceeding that of the initial condition and moves faster than the smaller wave. Since the oscillating tail disperses, the only ultimate evidence of the initial condition is two infinitely separated solitary waves.

As β increases from zero, the solitary waves increase in amplitude and decrease in bandwidth. Nearly all energy and momenta of the wave system remains with the solitary wave pair, but the portion accruing to the second wave increases as β increases. Consistent with this, the ratio of the amplitude of the second to first solitary wave increases with β. At some value $0{\cdot}1667 < \beta < 0{\cdot}2500$ that we have not located precisely, this deceleration of the solitary waves is catastrophic and the picture painted above becomes inapplicable, as the dispersive term in equation (1) in effect changes sign. Permanent waves are no longer possible. If, however, the sign of α (the coefficient of the nonlinear term) is reversed, the formation of a solitary wave and an oscillatory tail again proceeds, but with the opposite directions of propagation. These waves have speeds exceeding $\frac{1}{3}\alpha a$ and apparently more solitary waves emerge from the initial disturbance. This is not likely to be physically meaningful in the context of waves on concentrated vortices, for which k must be small.

This work was supported by N.A.S.A. Grant NGR 33-010-042, monitored by the Lewis Research Center.

Appendix

A quadrature formula representing the truncated integral must be chosen to avoid large errors near the singular point, since many quadrature formulae have errors that are proportional to derivatives of the integrand (kernel included, of course). The approximation used here results from integrating the integral exactly from $x_j - \frac{1}{2}h_x$ to $x_j + \frac{1}{2}h_x$, using a Taylor series expansion for $U_{\xi\xi\xi\xi}$ about the point $\xi = x_j$ and then replacing the derivative at x_j by finite-difference approximations. This leads to the single-step contribution (before the last step) from the jth grid point to the integral evaluated at the ith grid point of

$$h_x\, W(m)\,(U_{xxxx})_j^n,$$

where $m = i - j$ and

$$W(m) = \begin{cases} (m/|m|)\{\ln 2h_x - 1 + (|m| + \frac{1}{2})\ln(|m| + \frac{1}{2}) - (|m| - \frac{1}{2})\ln(|m| - \frac{1}{2})\}, & m \neq 0, \\ 0, & m = 0. \end{cases}$$

It is not difficult to show (Randall 1972) that the error to the quadrature involved in using this formula is $O(h_x^2 \ln h_x)$, as is the error due to omitting the singular point $\xi = x$.

REFERENCES

Gardner, C. S., Greene, J. M., Kruskal, M. D. & Miura, R. M. 1967 Method for solving the Korteweg–de Vries equation. *Phys. Rev. Lett.* **19**, 1095.

Leibovich, S. 1970 Weakly non-linear waves in rotating fluids. *J. Fluid Mech.* **42**, 803.

Pritchard, W. G. 1970 Solitary waves in rotating fluids. *J. Fluid Mech.* **42**, 61.

Randall, J. D. 1972 Ph.D. thesis, Cornell University.

Zabusky, N. J. 1968 Solutions and bound states of the time-independent Schrödinger equation. *Phys. Rev.* **168**, 124.